

Expulsion of Ions from Hydrophobic Hydration Shells

*Blake M. Rankin and Dor Ben-Amotz**

Department of Chemistry, Purdue University, 560 Oval Drive, West Lafayette, IN 47906, United States

SUPPORTING INFORMATION

This document contains additional descriptions of the methods used to obtain the results in the parent manuscript (Section I), as well as supplementary results which provide further validation of the conclusions reached in the parent manuscript (Section II).

I. EXPERIMENTAL, THEORETICAL, AND DATA ANALYSIS METHODS

Sodium fluoride (NaF, BioXtra, $\geq 99\%$), sodium iodide (NaI, ACS reagent, $\geq 99.5\%$), sodium formate (puriss. p.a., ACS reagent, Sigma Aldrich, $\geq 99.0\%$), sodium trimethylacetate (TMA⁻, Aldrich, 99%), tert-butylamine (TBNH₂, purified by redistillation, $\geq 99.5\%$), trimethylamine N-oxide (TMAO, 98%), tetramethylammonium fluoride (TMeA⁺F⁻, 97%), and tetramethylammonium iodide (TMeA⁺I⁻ ACS reagent, 99%) were obtained from Sigma-Aldrich. Deuterated (D9) tert-butyl alcohol (98%) and deuterated (D9) TMAO (98%) were purchased from Cambridge Isotope Laboratories, Inc. Solutions were prepared using ultrapure water (Milli-Q UF plus, Millipore, Inc.), with an electrical resistance of 18.2 M Ω ·cm. Solutions were all prepared with a maximum concentration of ~ 0.5 M for the molecular solute and 3 M for the salt, except when these concentrations were above the solubility limit. Thus, the maximum NaF

concentration was ~ 1 M and the TMeA^+I^- measurements were performed with maximum concentrations of 0.1 M TMeA^+I^- and 0.4 M NaI. The TMeA^+F^- measurements were performed with maximum concentrations of 0.1 M TMeA^+F^- and 0.9 M NaF. The TMA^- in NaF results were obtained using a solute concentration of 0.1 M.

Raman spectra were collected using a 514.5 nm Ar-ion laser with approximately 15 mW of power at the sample. The back-scattered stokes-shifted Raman photons were dispersed using a grating with 1200gr/mm, to obtain a spectral resolution of approximately 1 cm^{-1} in the CH stretch region. Raman spectra of deuterated solutes were collected using a 300gr/mm grating, with a spectral resolution of approximately 6 cm^{-1} in the CD stretch region. Duplicate spectra were collected with accumulation times of 0.2 seconds integrated over 5 minutes. Self Modeling Curve Resolution (SMCR)¹ was implemented using IGOR Pro (WaveMetrics Version 6.2.2.2). Previously, we have shown that three component solutions consisting of water, ions, and tert-butyl alcohol (TBA) can be reduced to two component systems.² The same experimental strategy is employed in this work. CH frequency shifts were calculated by fitting the symmetric CH stretches to Gaussian functions. The resulting frequencies were fit using a linear function to determine the slope of the shift ($\text{cm}^{-1}/\text{M NaI}$). The average of three independent data sets is reported in Table S1.

Extrapolation was used to obtain the 0 M NaI CH frequencies of TMeA^+ in Figures 1 and 3 of the parent manuscript. This was necessary since TMeA^+ solutions contained either fluoride or iodide counterions. Therefore, a linear regression was applied to the CH frequencies of TMeA^+ fluoride or iodide to obtain the CH frequency at 0 M NaF or NaI.

Mulliken Population³ and Natural Population Analysis⁴ methods at the HF/6-31++G(d,p) and DFT/6-31++G(d,p) levels of theory using Gaussian 09 were used to calculate the partial charge

on the methyl groups, which were obtained from the sum of the partial charges on the carbon and three hydrogen atoms. The average of these charges is reported in Table S1.

Estimation of the Cut-Off Between the Ion Affinity and Expulsion Regimes

If we assume that the concentration of iodide in the first hydration shell of TMAO (and the other molecular solutes) is equivalent to the iodide concentration in the surrounding aqueous solution, then we may obtain the following approximate expression for the concentration of solutes whose first hydration shells contain an Γ ion.

$$[SI^-] = [S]_0 N_{SI} \approx [S]_0 \left(N_{HS} \frac{[\Gamma^-]_0}{[W]_0} \right) = \frac{N_{HS} [S]_0 [\Gamma^-]_0}{[W]_0} \quad (S1)$$

N_{SI} is the number of Γ ions in the first hydration shell of the solute, $N_{HS} \sim 17$ is the number of water molecules in the first hydrophobic hydration shell of the TBA and TMAO,⁵ $[W]_0 \sim 55.5$ M is the concentration of pure water, $[S]_0 = [S] + [SI^-]$ is the total solute concentration, and $[\Gamma]_0 = [\Gamma] + [SI^-]$ is the total concentration of Γ . Note that the second (approximate) equality in Eq. S1 is obtained by equating the ratio of the number of ions to the number of water molecules in the hydration shell with the corresponding bulk concentration ratio $N_{SI}/N_{HS} = [\Gamma]_0/[W]_0$, so $N_{SI} = N_{HS} ([\Gamma]_0/[W]_0)$. We may use Eq. S1 to predict the fraction of solute molecules whose hydration shells contain Γ .

$$f = \frac{[SI^-]}{[S]_0} \approx \frac{N_{HS} [\Gamma^-]_0}{[W]_0} \quad (S2)$$

Note that f is equivalent to the average number of ions in the solute's hydration shell, and so the predicted values of f can be larger than one at sufficiently high Γ concentrations.

Equation 2 in the parent manuscript is equivalent to the following expression for K_A .

$$K_A = \frac{[SI^-]}{[S][I^-]} = \frac{[SI^-]}{\{[S]_0 - [SI^-]\} \{[I^-]_0 - [SI^-]\}} \quad (\text{S3})$$

We may combine the above Eqs. S2 and S3 to obtain the following approximate expression for the cut-off value of K_A pertaining to a situation in which local I^- concentration in the first hydration shell of the solute is the same as the bulk I^- concentration.

$$K_A \approx \frac{f[S]_0}{([S]_0 - f[S]_0)([I^-]_0 - f[S]_0)} = \frac{\frac{N_{HS}[S]_0[I^-]_0}{[W]_0}}{\left\{ [S]_0 - \frac{N_{HS}[S]_0[I^-]_0}{[W]_0} \right\} \left\{ [I^-]_0 - \frac{N_{HS}[S]_0[I^-]_0}{[W]_0} \right\}} \quad (\text{S4})$$

Thus, when $[S]_0 \sim 0.5$, $[I^-]_0 \sim 1\text{M}$ we obtain $K_A \sim 0.5 \text{ M}^{-1}$, while when $[I^-]_0 \sim 3\text{M}$ we obtained $K_A \sim 4.5 \text{ M}^{-1}$. The reason that these predicted K_A cut-off value depend on $[I^-]_0$ is that Eq.S 2 implies that f is linearly proportional to $[I^-]_0$ while the binary aggregation equilibrium expression for K_A implies a non-linear dependence of f on $[I^-]_0$. Nevertheless, the predictions obtained using Eq. S3 are generally consistent with the conclusion that a true affinity between an ion and a molecular solute would produce an equilibrium constant greater than $\sim 1 \text{ M}^{-1}$.

II. SUPPLEMENTARY RESULTS

Methyl Group CH Frequency Shifts and Partial Charges

Table S1. Iodide-induced CH frequency shifts and calculated partial charges.

Solute	CH Frequency Shift ($\text{cm}^{-1}/\text{M NaI}$)	Partial Charge per Methyl Group
TMA ⁻	-0.46 ± 0.01	-0.10 ± 0.13
TBNH ₂	-0.70 ± 0.03	-0.02 ± 0.05
TBA	-0.92 ± 0.04	-0.01 ± 0.03
TMAO	-1.54 ± 0.04	$+0.26 \pm 0.03$
TMeA ⁺	-2.98 ± 0.14	$+0.37 \pm 0.04$

Table S1 contains the slopes of the best fit CH frequency shift lines shown in Figure 3A of the parent manuscript, and the corresponding methyl group partial charges obtained as described above.

CH Frequency Shift Polarization Analysis

The CH frequency shifts reported in Table S1 originate from the symmetric CH stretch of the unpolarized spectra. The magnitude of the shift is independent of polarization in that the same slope ($\text{cm}^{-1}/\text{M NaI}$) is obtained from the symmetric stretch of the unpolarized and isotropic Raman⁶, which is defined as:

$$Iso = V - \frac{4}{3}H$$

Polarized Raman spectra were collected by coupling a polarizing beam splitter with a Soleil-Babinet Compensator (Special Optics) to rotate the laser polarization.

Fluoride-Correlated Spectra

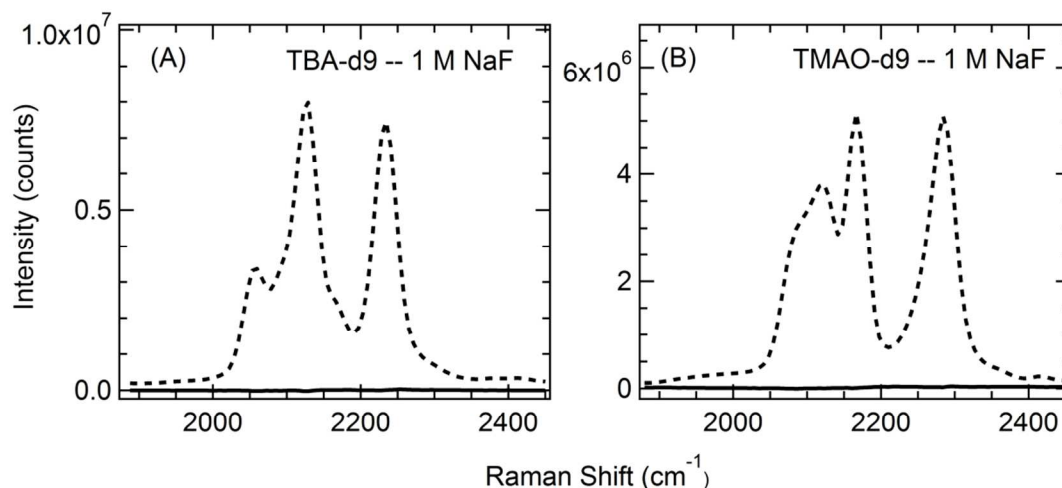


Figure S1. Fluoride-correlated spectra in aqueous TBA-d9 (A) and TMAO-d9 (B) solvents.

Figure S1 displays the ion-correlated spectra of 1 M NaF in aqueous TBA-d₉ (A) and TMAO-d₉ (B) solvents, in the CD stretching band region (obtained in the same way as those of Figure 4 in the parent manuscript). The nearly flat (approximately zero area) solid curves in panels A and B confirm that there are no F⁻ ions in the first hydration shells of TBA or TMAO.

Ion-Correlated Spectra Obtained using a Two-Step Analysis Procedure

The following two-step analysis procedure was implemented to obtain ion-correlated spectra from aqueous solutions containing non-deuterated molecular solutes. Figure S2(A) shows the SC spectra of TBA in water and TBA in 1 M NaI, obtained using SMCR in the same way as those shown in Figures 1 and 2 of the parent manuscript. The spectra shown in Figure S2(B) were obtained by performing a second SMCR analysis on the CH stretch band region of the SC spectra shown in Figure S2(A). More specifically, the two CH bands in Figure S2(A) that pertain to solutions with either 0 M or 1 M NaI were used to obtain ion-correlated CH spectral components.

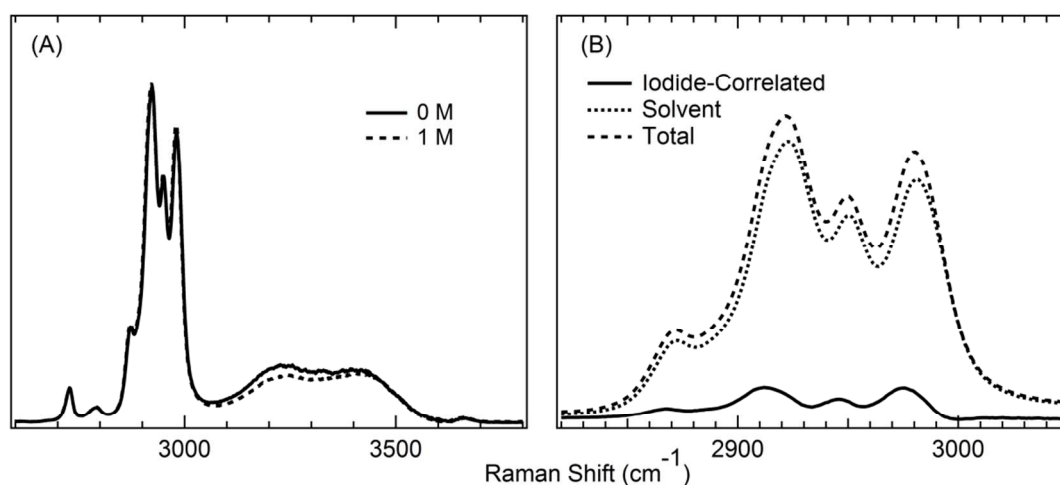


Figure S2. Solute-correlated (SC) spectra of TBA in water and 1 M NaI (A). These spectra are decomposed into the I⁻-correlated component shown in (B).

The results shown in Figure S2(B) indicate that the Γ -correlated CH band of TBA is red-shifted approximately 10 cm^{-1} relative to the solvent component (associated with salt free aqueous TBA). Similar results are obtained for other molecular solutes, as both TBA and TMAO yield ion-correlated CH shifts of $9 \pm 3\text{ cm}^{-1}$. We have further demonstrated that the latter shifts are independent of Γ concentration (as discussed below).

Independence of Iodide-Correlated CD shift and Iodide Concentration

The magnitude of the CH and CD frequency shifts in the Γ -correlated spectra are found to be independent of Γ concentration. The Γ -correlated TBA CH shifts shown in Figure S3 were obtained in the same way as those shown in Figure 4 of the parent manuscript with different NaI concentrations. The data point at 0 M NaI corresponds to the CH frequency of TBA in water.

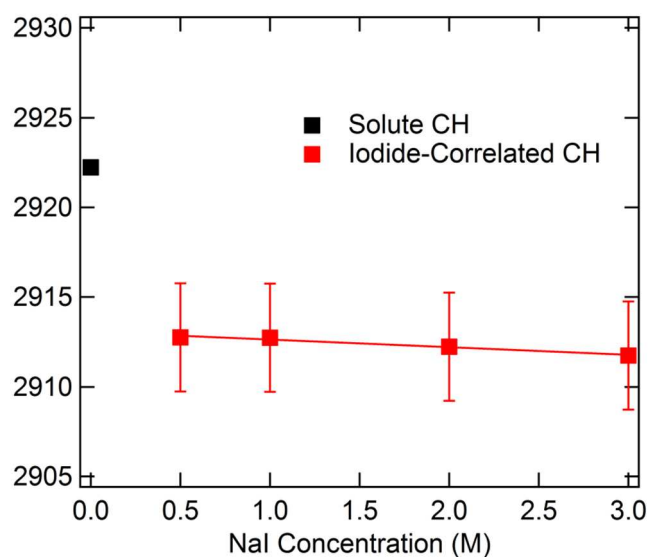


Figure S3. CH frequency shifts in the iodide-correlated spectra.

The fact that the CH shift does not change with increasing Γ concentration implies that the observed ion-correlated shift arises from those TBA molecules whose hydration shells contain a single Γ ion. In other words, if the observed ion-correlated shift were due to a single ion when

the salt concentration is low but more than one ion when the salt concentration is high, then we would have expected to observe a different ion-correlated shift at different salt concentrations. Although the ion-correlated CH shift does not change with Γ concentration, the number of perturbed TBA molecules (obtained from the area of the ion-correlated CH band) is found to scale linearly with Γ concentration. In other words, the fraction of perturbed solute molecules increases in direct proportion to the concentration of Γ .

Further evidence supporting our conclusion that Γ is expelled from the hydration shell of TBA and TMAO is provided below, in the sub-section entitled *Additional Evidence for the Expulsion of Ions From Hydrophobic Hydration Shells*.

Evaluation of f from Solute CH Frequency Shifts

The fraction of solute molecules with an Γ in the first hydration shell, f , is shown in Figure S4 for TMA⁻, TBNH₂, TBA, TMAO, and TMeA⁺. These values were obtained from the Γ -induced CH frequency shifts in the molecular solute-correlated spectra. Note that the CH shifts in the Γ -correlated spectra are independent of Γ concentration (discussed above); therefore, the magnitude of the shifts shown in Figure 3 of the parent manuscript represent differences between the number of Γ ions in the corresponding hydrophobic hydration shell. Thus, f is expected to be approximately equivalent to the ratio of the CH shifts shown in Figure 3 of the parent manuscript divided by the CH shift of $9 \pm 3 \text{ cm}^{-1}$ pertaining to solutes whose hydration shells contain a single Γ ion. Equation S2 was used to produce the dashed trace, assuming that $N_{\text{HS}} = 17$ for TBA.

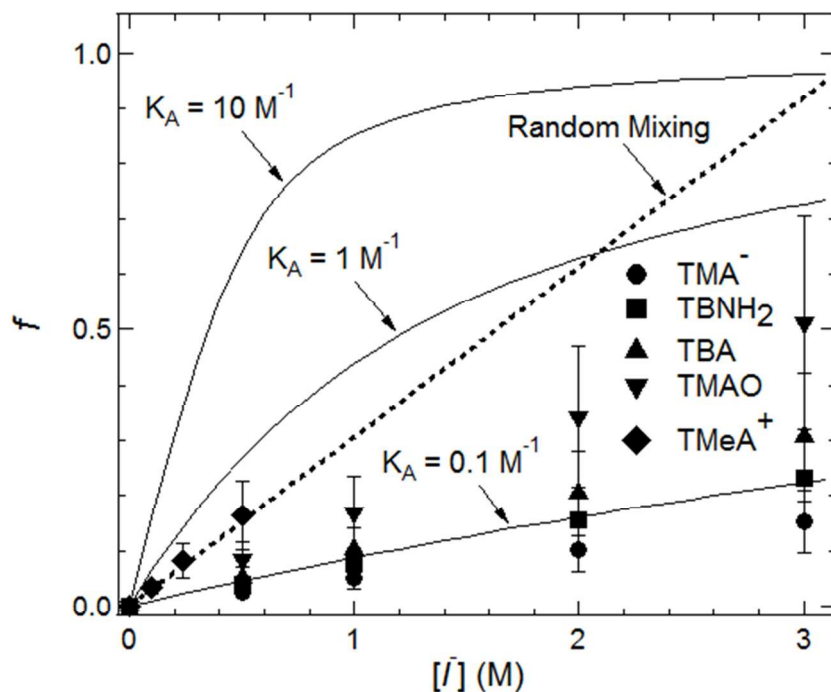


Figure S4. Fraction of solute molecules with an I^- in the hydration shell as a function of $[I^-]$ for TMA^- , $TBNH_2$, TBA , $TMAO$, and $TMeA^+$. The error bars on the points in this figure were obtained from the calculation of f using 6 and 12 cm^{-1} as the frequency shift associated with having an I^- in the hydrophobic hydration shell.

Effect of Solute Concentration

The following measurements were performed in order to demonstrate that the SC spectral changes and CH frequency shifts in Figure 3 of the parent manuscript are due to penetration of I^- into the hydration shell of the molecular solutes, rather than to salt induced aggregation of the molecular solutes. If the observed SC CH shifts were due to salt induced aggregation then one would expect the observed shifts to depend on the concentration of the molecular solute. To verify that this is not the case we have reduced the concentration of TBA and TMAO by a factor of five, from 0.5 M to 0.1 M, and observed essentially identical SC spectra. More specifically, Figure S5 compares the CH frequency shifts obtained at the two TBA and TMAO concentrations, plotted as a function of NaI concentration. The 0.5 M TBA data was reported

previously² and is included here for comparison. The fact that the slope of the CH frequency shift vs. NaI concentration is identical (within experimental error) for both 0.1 and 0.5 M TBA (and TMAO) confirms that the observed shifts are not due to aggregation of the solute.

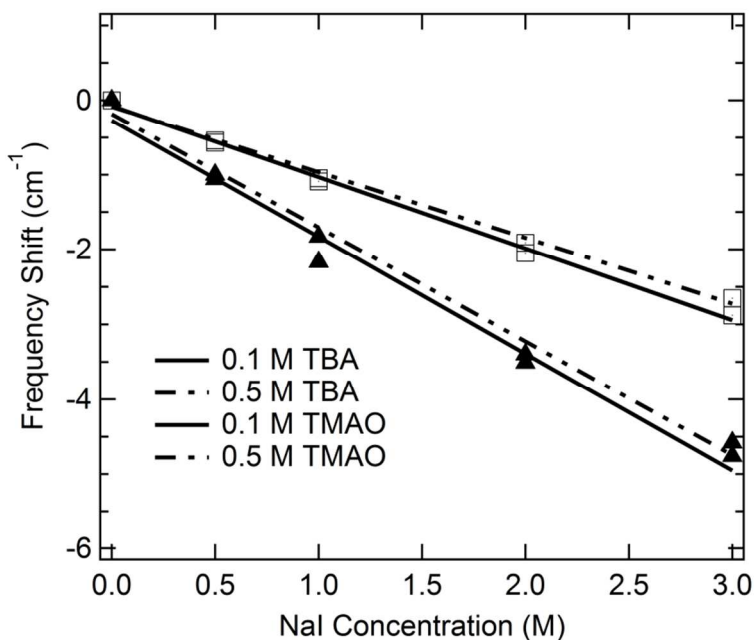


Figure S5. Iodide-induced CH frequency shifts of 0.1 and 0.5 M TBA and TMAO.

Absence of Ion Pairing

To exclude the possibility that Na^+ and I^- form ion pairs as NaI concentration increases, we have obtained the SC spectra of NaI in water. These spectra are shown in Figure S6. The dashed blue curve corresponds to the OH band of bulk water. The solid curves display the OH bands obtained from the ion-correlated spectra of NaI in water (with no molecular solutes). If Na^+ and I^- formed ion pairs, a depletion of the hydration shell of I^- would be observed. The fact that the area under the solid curves scales linearly with NaI concentration (Panel B) indicates that iodide maintains its full hydration shell throughout this concentration range. Thus, the results shown in the parent manuscript are not influenced by either direct-contact ion pairing or ion-pairs

separated by a single water layer, as formation of either of the latter ion-pairs would have produced a non-linear concentration dependence.

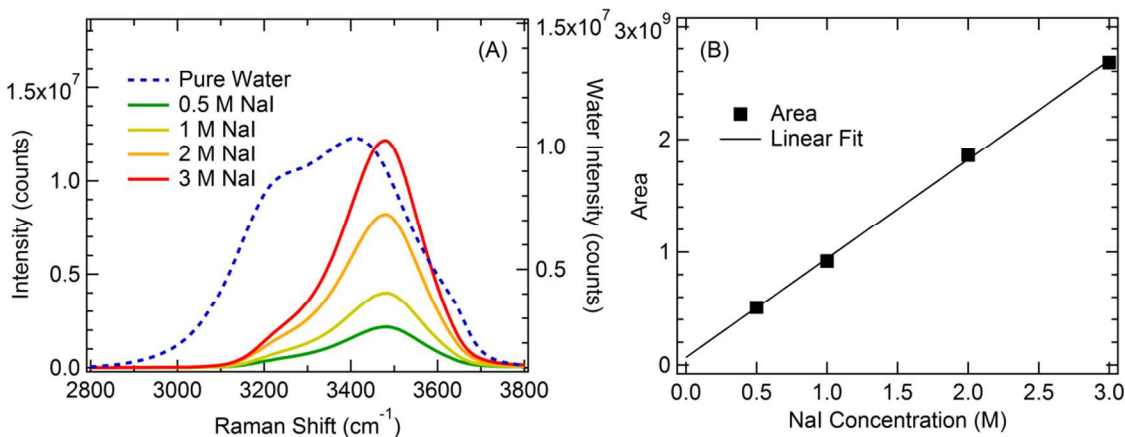


Figure S6. Solute-correlated (SC) spectra of NaI in water (A). The integrated areas under the curves shown in (A) scale linearly with concentration (B).

Suppression of Ion Hydration Shell and Solute Head Group Contributions to SC Spectra

Hydration shell spectra obtained from solutions containing molecular solutes and salts may contain features arising both from the molecular and ionic hydration shells, as well as contributions from the molecular polar head groups. The following describes a Raman-MCR strategy that we have found to be quite effective in separating the latter contributions. However, it is important to note that the CH and CD frequency shift results reported in this work are independent of whether or not these ion hydration shell and polar head group contributions are or are not separated from the hydrophobic hydration shell contributions to SC spectra.

Two-component Raman-MCR analyses of solutions containing both molecular solutes and salts, when performed using a solvent spectrum obtained from pure water, yield SC spectra whose OH region may be dominated by a feature arising from water molecules that are H-bonded to the anion. For example, the solid black curve in Figure S7 shows such a SC spectrum

obtained from a solution containing 0.5M TBA and 3M NaI – the OH band peaked near 3500 cm^{-1} is that associated with water molecules that are H-bonded to I^- .² The latter feature may be effectively suppressed simply by adding an appropriate concentration of NaI to the pure solvent spectrum, so that both solutions contain the same concentration of I^- (and the Na^+ is not problematic as it has little influence on the SC spectrum of water²). When SMCR is performed in this way, then the SC spectrum of the molecular solute contains features that arise from the hydration shell of the molecular solute, and look quite similar to the corresponding hydration shell spectra of the same molecular solute in pure water. The red curves in Figure S7(A) and (C) show such SC spectra, obtained from a solution containing 0.5 M TBA and 3 M NaI and a solvent containing 3 M NaI.

A similar procedure may be used to remove the anionic carboxylate head group contribution from the SC spectra of TMA^- . This can be done by adding an equal concentration of sodium formate to the solvent. Thus, the resulting SC spectra will not contain features arising from the direct interaction of water with the carboxylate head group of TMA^- , and so any remaining SC features will arise predominantly from interactions of water with the hydrophobic trimethyl group of TMA^- . Figures S7(B) and (D) show TMA^- SC spectra obtained using either pure water (purple curve) or aqueous sodium formate as the solvent (magenta curve). Thus, the purple SC spectra contains a higher frequency OH feature arising in part from the interaction of water with the carboxylate head group, while the magenta SC spectrum contains a SC OH band that arises primarily from the hydrophobic hydration shell of TMA^- .

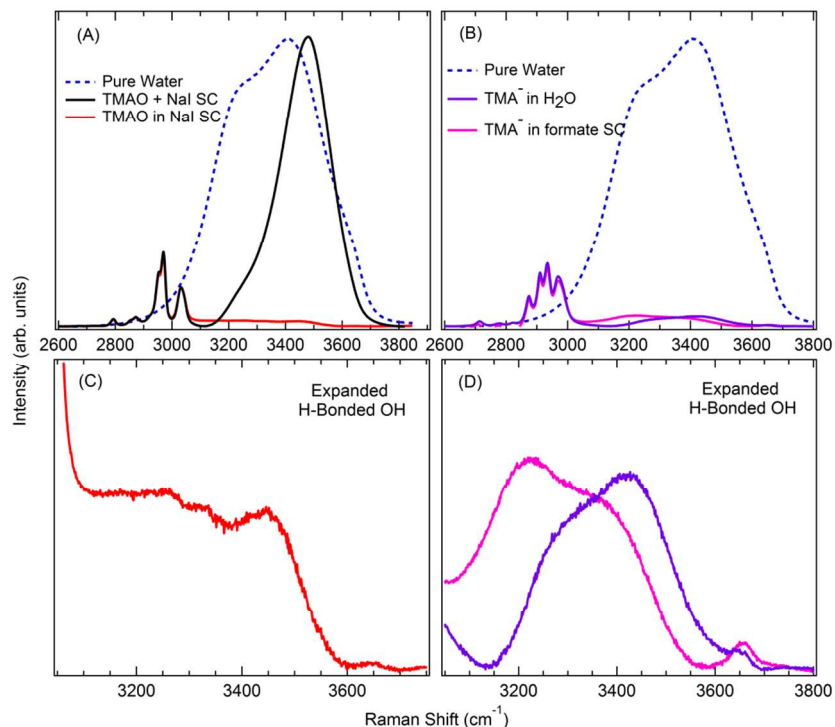


Figure S7. Solute-correlated (SC) spectra of TMAO in a water solvent and in an aqueous solution of 3 M NaI (A). Solute-correlated (SC) spectra of TMA⁻ in a water solvent and in an aqueous NaI solution (B). The dashed blue curves in (A) and (B) correspond to bulk water. Expanded CH and OH region of TMAO (C) and TMA⁻ (D).

Additional Evidence for the Expulsion of Ions From Hydrophobic Hydration shells

Our conclusion that I⁻ is expelled from hydrophobic hydration shells is supported both by the linear concentration dependence of the frequency shifts shown in Figure 3 of the parent manuscript, as well as by the evidence described above, in the sub-section entitled *Independence of Iodide-Correlated CD shift and Iodide Concentration*. The following results provide further support for our conclusion that I⁻ ions are expelled from the hydration shells of TBA.

If there were a true affinity between a molecular solute and a given ion then one would expect the hydration shell of the ion to contain fewer water molecules than it does when the ion is dissolved in pure water. Figure S8 shows the OH stretch bands in the SC spectra of I⁻ obtained in pure water (dashed curves) and in an aqueous solution containing 0.5 M TBA. The very slight

reduction in the area of the latter SC spectra is consistent with a reduction in the concentration of water when adding TBA. Thus, these results confirm that the Γ ions remain essentially fully hydrated after TBA is added, and thus Γ ions do not have a significant affinity for TBA. Similar results are obtained for the other solute molecules shown in Figure 3 of the parent manuscript.

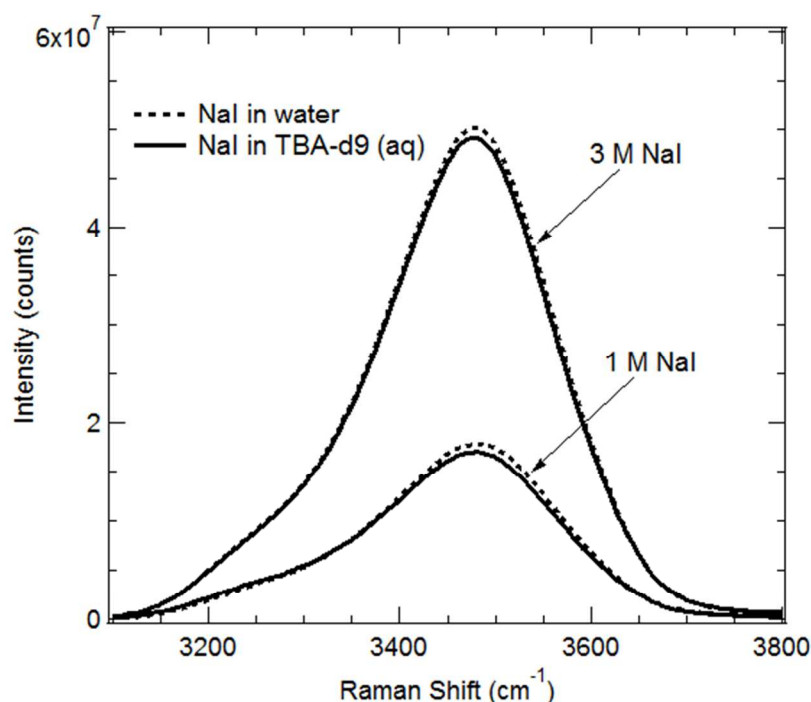


Figure S8. This figure shows the OH stretch bands obtained from the SC spectra of Γ in pure water (dashed curves) and 0.5 M aqueous TBA (solid curves). The similar areas of the dashed and solid bands confirm that Γ does not have a high affinity for TBA (see text for further details).

Rotational Ambiguity: Lower and Upper Bounds

The SC spectra shown in the parent manuscript represent lower bound SC spectra as they are equivalent to the minimum area non-negative SC spectra obtained when subtracting the measured spectrum of pure solvent from that of the solution of interest.⁷ Other mathematically acceptable SC spectra can be obtained by subtracting less of the solvent spectrum from the solution spectrum, leading to an upper bound on the SC spectrum that is equivalent to the

experimentally measured spectrum of the solution with the highest solute concentration. The latter upper bound is equivalent to assuming that at the highest solute concentration all the molecules in the solution are in the solvation shell of a solute molecule. Although this upper bound represents a mathematically feasible SC spectrum, it may not be physically reasonable.

The lower bound SC spectra obtained in the parent manuscript (such as those shown in Figure 4) imply that the CH (or CD) frequency red-shift induced by a single first hydration shell Γ ion is $9 \pm 3 \text{ cm}^{-1}$. Previous hybrid quantum-classical calculations predicted an Γ -induced CH red-shift of TBA of $4 \pm 1 \text{ cm}^{-1}$ (and a range of $\sim 2 \text{ cm}^{-1}$ to $\sim 6 \text{ cm}^{-1}$).² The latter predicted frequency shift may be used to obtain physically reasonable upper bound values for f and K_A , as shown in Table S2.

Table S2. Values of f and K_A for all molecular solutes at $[\Gamma]_0 = 1 \text{ M}$.

		Frequency Shift when an Γ ion is in the first hydration shell	
		9 cm^{-1}	4 cm^{-1}
TMA⁻	f	0.05	0.12
	K_A	0.06	0.14
TBNH₂	f	0.08	0.18
	K_A	0.09	0.23
TBA	f	0.10	0.23
	K_A	0.12	0.33
TMAO	f	0.17	0.39
	K_A	0.23	0.78
TMeA⁺ (0.1 M)	f	0.33	0.75
	K_A	0.51	3.16

For example, our observed CH frequency shift of 1.54 cm^{-1} for TMAO in 1 M aqueous NaI implies that there is a lower bound probability of ~ 0.17 ($f = 1.54/9 = 0.17$) and upper bound

probability of ~ 0.39 ($f = 1.54/4 = 0.39$) of finding a single Γ ion in the first hydration shell of TMAO. Table S2 contains f values obtained in this way, along with the corresponding K_A values obtained using Eq. 2 of the parent manuscript, for TMAO and the other molecular solutes. These indicate that the upper bound estimates (obtained assuming the 4 cm^{-1} shift value) imply that Γ may have a slight affinity for TMeA^+ while the local Γ concentration around TMAO may be near the random mixing limit. However, both our lower and upper bound results indicate that Γ is expelled from the hydration shells of TMA^- , TBH_2 , and TBA.

REFERENCES

- (1) Lawton, W. H.; Sylvestre, E. A. *Technometrics* **1971**, *13*, 617.
- (2) Rankin, B. M.; Hands, M. D.; Wilcox, D. S.; Fega, K. R.; Slipchenko, L. V.; Ben-Amotz, D. *Faraday Discuss.* **2013**, *160*, 255.
- (3) Mulliken, R. S. *J. Chem. Phys.* **1955**, *23*, 1833.
- (4) Reed, A. E.; Weinstock, R. B.; Weinhold, F. *J. Chem. Phys.* **1985**, *83*, 735.
- (5) Fornili, A.; Civera, M.; Sironi, M.; Fornili, S. L. *Phys. Chem. Chem. Phys.* **2003**, *5*, 4905.
- (6) Walrafen, G. E. *J. Chem. Phys.* **2005**, *122*, 174502.
- (7) Fega, K. R.; Wilcox, D. S.; Ben-Amotz, D. *Appl. Spectrosc.* **2012**, *66*, 282.